

PP4 is a γ H2AX phosphatase required for recovery from the DNA damage checkpoint

Shinichiro Nakada¹, Ginny I. Chen^{1,2}, Anne-Claude Gingras^{1,2+} & Daniel Durocher^{1,2++}

¹Centre for Systems Biology, Samuel Lunenfeld Research Institute, Mount Sinai Hospital, and ²Department of Molecular Genetics, University of Toronto, Toronto, Ontario, Canada

 This is an open-access article distributed under the terms of the Creative Commons Attribution License, which permits distribution, and reproduction in any medium, provided the original author and source are credited. This license does not permit commercial exploitation or the creation of derivative works without specific permission.

Phosphorylation of histone H2AX on Ser 139 (γ H2AX) is one of the earliest events in the response to DNA double-strand breaks; however, the subsequent removal of γ H2AX from chromatin is less understood, despite being a process tightly coordinated with DNA repair. Previous studies in yeast have identified the Pph3 phosphatase (the PP4C orthologue) as important for the dephosphorylation of γ H2AX. By contrast, work in human cells attributed this activity to PP2A. Here, we report that PP4 contributes to the dephosphorylation of γ H2AX, both at the sites of DNA damage and in undamaged chromatin in human cells, independently of a role in DNA repair. Furthermore, depletion of PP4C results in a prolonged checkpoint arrest, most likely owing to the persistence of mediator of DNA damage checkpoint 1 (MDC1) at the sites of DNA lesions. Taken together, these results indicate that PP4 is an evolutionarily conserved γ H2AX phosphatase.

Keywords: DNA damage checkpoint; protein phosphatases; DNA damage; H2AX; PP4

EMBO reports (2008) 9, 1019–1026. doi:10.1038/embor.2008.162

INTRODUCTION

In response to DNA double-strand breaks (DSBs), the histone H2A variant H2AX is rapidly phosphorylated by the phosphatidylinositol(3) kinase-like kinases ATM, DNA-PKcs and ATR (ataxia telangiectasia mutated, DNA-dependent protein kinase catalytic subunit and ataxia telangiectasia and Rad3 related, respectively) to form γ H2AX (Rogakou *et al*, 1998). This phosphorylation event

produces a large chromatin domain of up to 1 Mb surrounding DNA lesions, which acts as a signal for the recruitment and accumulation of DNA repair and signalling proteins (Rogakou *et al*, 1999; Celeste *et al*, 2003). For example, the checkpoint mediator MDC1 (mediator of DNA damage checkpoint 1) binds to γ H2AX directly through an interaction between the MDC1 tandem BRCT domains and an H2AX epitope encompassing phosphoserine 139 and its free carboxyl terminus (Stucki *et al*, 2005). The γ H2AX–MDC1 complex, in turn, promotes the recruitment of many proteins such as 53BP1 (tumour protein p53-binding protein 1), NBS1 (Nijmegen breakage syndrome 1), RNF8 (ring-finger protein 8) and BRCA1 (breast cancer 1 early onset) to mediate DNA repair and checkpoint signalling (Harper & Elledge, 2007).

Although the formation of γ H2AX and its role in promoting protein recruitment to the sites of DNA damage are becoming increasingly understood, much less is known about how and why it is removed from chromatin once DNA repair has been effected. The removal of γ H2AX from sites of DNA damage is evidently tightly regulated, as it is closely correlated with DNA repair. Mechanisms must therefore exist to restrict γ H2AX to sites of DNA lesions. These systems most likely comprise phosphatases that erase the γ H2AX histone marker and histone/nucleosome remodelling activities that remove γ H2AX from sites of DNA damage (Linger & Tyler, 2007). How these two processes integrate together is so far not understood.

Work in budding yeast recently identified the product of the *PPH3* gene as the sole γ H2AX phosphatase in this organism (Keogh *et al*, 2006). Pph3 encodes the orthologue of the mammalian PP4 phosphatase catalytic subunit (PP4C; Cohen *et al*, 1990; Ronne *et al*, 1991; Brewis *et al*, 1993). The yeast PP4 complex does not seem to have a direct function in DNA repair but rather acts to couple DSB repair with termination of checkpoint signalling, a process commonly referred to as checkpoint recovery (Keogh *et al*, 2006). The role of Pph3 in checkpoint recovery is at least in part due to its function as a γ H2AX phosphatase, as the delay in checkpoint recovery manifested by *pph3 Δ* cells is largely alleviated by the expression of a non-phosphorylatable H2A mutant (Keogh *et al*, 2006). Taken together,

¹Centre for Systems Biology, Samuel Lunenfeld Research Institute, Mount Sinai Hospital, 600 University Avenue, Toronto, Ontario M5G 1X5, Canada

²Department of Molecular Genetics, University of Toronto, 1 King's College Circle, Toronto, Ontario M5S 1A8, Canada

+Corresponding author. Tel: +1 416 586 4800 ext 5027; Fax: +1 416 586 8857; E-mail: gingras@mshri.on.ca

++Corresponding author. Tel: +1 416 586 4800 ext 2544; Fax: +1 416 586 8869; E-mail: durocher@mshri.on.ca

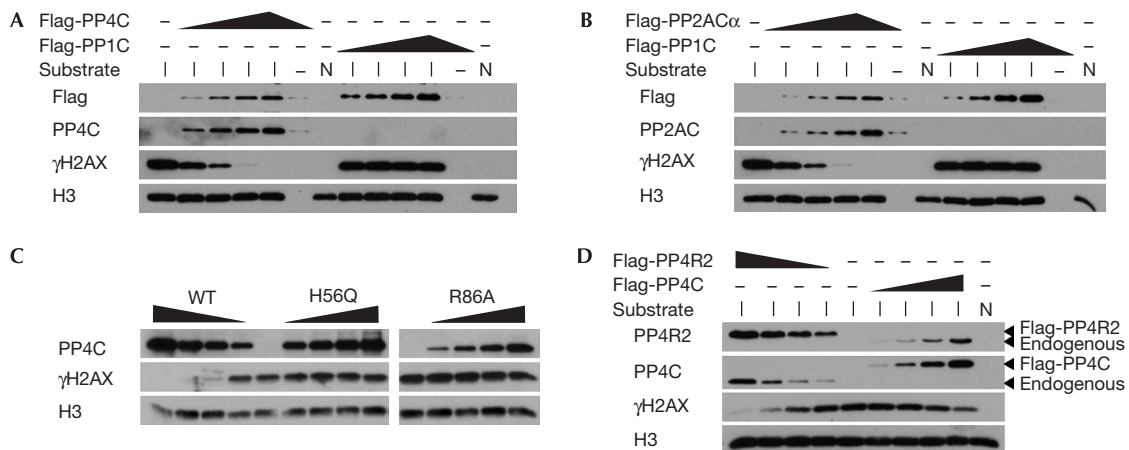


Fig 1 | PP4C and PP2AC α dephosphorylate H2AX *in vitro*. (A–D) Purified histone substrates isolated from cycling (N) or irradiation-treated U2OS cells (I) were incubated with varying amounts of immunopurified wild-type (WT) Flag-PP4C (A,C,D), Flag-PP2AC α (B), Flag-PP1C (A,B), phosphatase-dead Flag-PP4C-H56Q and PP4C-R86A mutants (C) and Flag-PP4R2 (D). Phosphatase reactions were followed by immunoblotting and probed with the indicated antibodies. H3, histone H3.

these results indicate that the formation of the γ H2AX chromatin domain and its dissolution are important in the control of checkpoint signalling. By contrast, recent work in human cells attributed the function of γ H2AX phosphatase to PP2A rather than PP4 (Chowdhury *et al*, 2005), raising doubts about the function of PP4 in the dephosphorylation of γ H2AX in species other than yeast.

Here, we address directly whether PP4 contributes to the dephosphorylation of γ H2AX in human cells. First, we show that immunopurified PP4 readily dephosphorylates γ H2AX *in vitro*. Depletion of PP4C by RNA interference in cycling or irradiated cells results in increased steady-state levels of γ H2AX. Furthermore, depletion of PP4C slows down the turnover of γ H2AX after the pharmacological inhibition of ATM and DNA-PK, indicating that PP4C is a physiological γ H2AX phosphatase. Consistent with this idea, depletion of PP4C results in persistent γ H2AX foci-positive cells, suggesting that PP4 acts at the sites of DNA damage. Intriguingly, dissolution of γ H2AX foci in PP4C-depleted cells is nevertheless observed 6 h post-irradiation despite the persistence of phosphorylated H2AX in the chromatin fraction. These results indicate that PP4 counteracts γ H2AX not only at the sites of DNA damage but also in undamaged chromatin. Finally, we observe a checkpoint recovery defect associated with the depletion of PP4C, suggesting that PP4 has a function in the termination of checkpoint signalling. Taken together, these results indicate that PP4 is an authentic γ H2AX phosphatase important for the spatio-temporal regulation of the DNA damage checkpoint.

RESULTS AND DISCUSSION

Immunopurified PP4 and PP2A dephosphorylate γ H2AX

In yeast, Pph3 encodes the yeast orthologue of human PP4C, which is part of a protein complex composed of Pph3, Psy2 and Psy4 (Gavin *et al*, 2002; Ho *et al*, 2002; Gingras *et al*, 2005). This complex is conserved in human cells and contains, in addition to PP4C, the PP4R2 and PP4R3 regulatory subunits. As PP2A rather than PP4 has been implicated as a mammalian γ H2AX phosphatase, we sought to determine whether human PP4 can also dephosphorylate γ H2AX. First, we tested whether purified PP4 dephosphorylates γ H2AX *in vitro*. For this purpose, we

acid-extracted histones from U2OS cells irradiated with a dose of 100 Gy to obtain histone preparations enriched in γ H2AX (supplementary Fig S1 online). As a source of phosphatases, we immunopurified epitope-tagged PP1C, PP2AC α , PP4C or the catalytically inactive PP4C-H56Q and PP4C-R86A mutants from stably transfected 293 cells where the expression of epitope-tagged PP2AC α and PP4C was found to be near wild-type levels (supplementary Fig S2 online). We opted to immunopurify protein phosphatase complexes rather than to purify free catalytic subunits to retain as much as possible the subunit composition of the PP2A and PP4 holoenzyme complexes. This approach is important to minimize a well-known loss of substrate specificity seen with isolated catalytic subunits (Tung *et al*, 1985), as their regulatory proteins allow the Ser/Thr phosphatases to interact with various targets under appropriate regulation. By using the criterion of activity against 6,8-difluoro-4-methylumbelliferyl phosphate, all wild-type phosphatase complexes were found to be active, whereas the catalytically inactive PP4C mutants had negligible activity (supplementary Fig S2 online). As shown in Fig 1, PP2AC α can readily dephosphorylate γ H2AX, as reported previously (Chowdhury *et al*, 2005). Furthermore, PP4C—but neither PP1 nor the PP4C phosphatase-dead mutants—also robustly dephosphorylates γ H2AX in a dose-dependent manner (Fig 1A–C). Finally, we immunoprecipitated epitope-tagged PP4R2, the orthologue of yeast Psy4, as a means of immunopurifying PP4C in complex with regulatory subunits. As shown in Fig 1D, immunoprecipitates of PP4R2 are able to dephosphorylate γ H2AX robustly to a level that is at least equivalent to immunopurified PP4C. From these results, we conclude that PP4C acts as a γ H2AX phosphatase *in vitro*.

PP4 and PP2A counteract phosphorylation of H2AX

Next, we examined the impact of PP4C and PP2AC depletion on the total levels of γ H2AX. We transfected small interfering RNA (siRNA) duplexes to deplete PP4C or PP2AC from U2OS cells (Fig 2A). As PP2AC is encoded by two genes in the human genome, giving rise to two proteins— α and β —that are 97% identical to each other (Zhou *et al*, 2003), our targeting duplexes

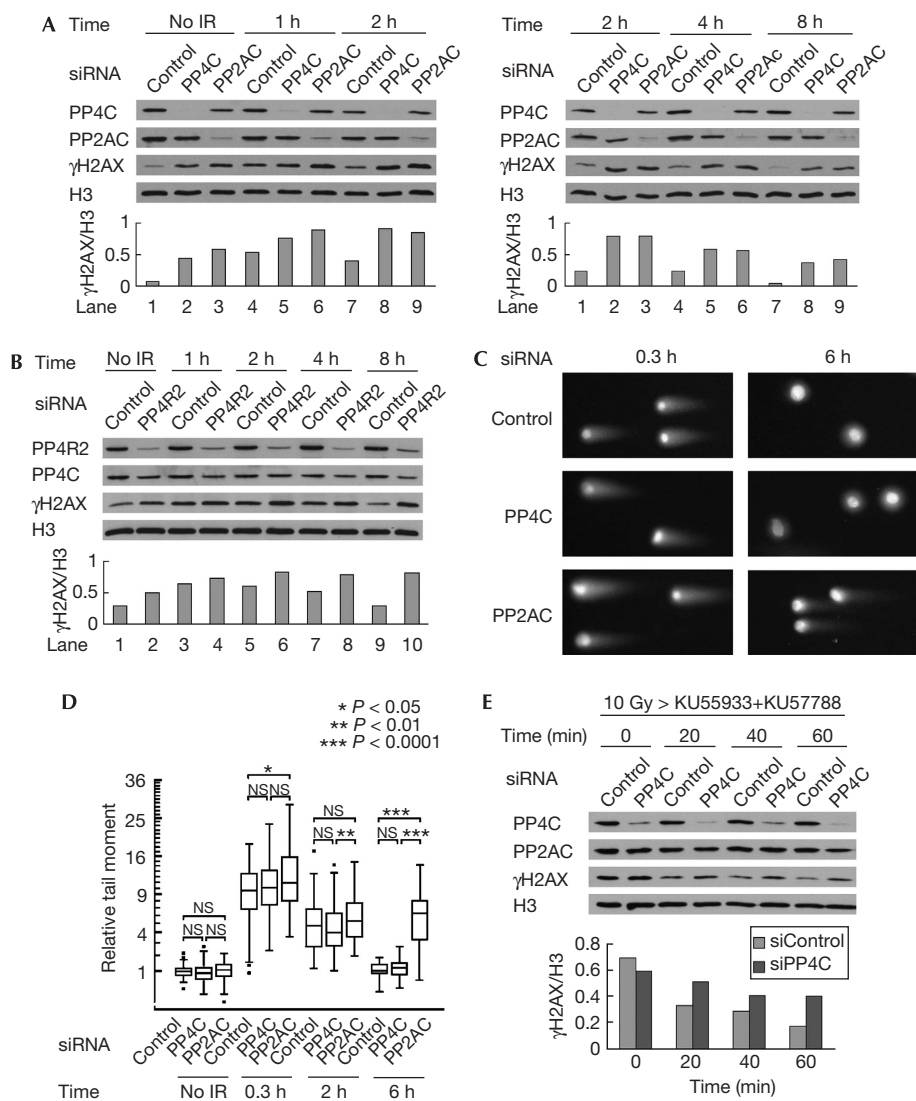
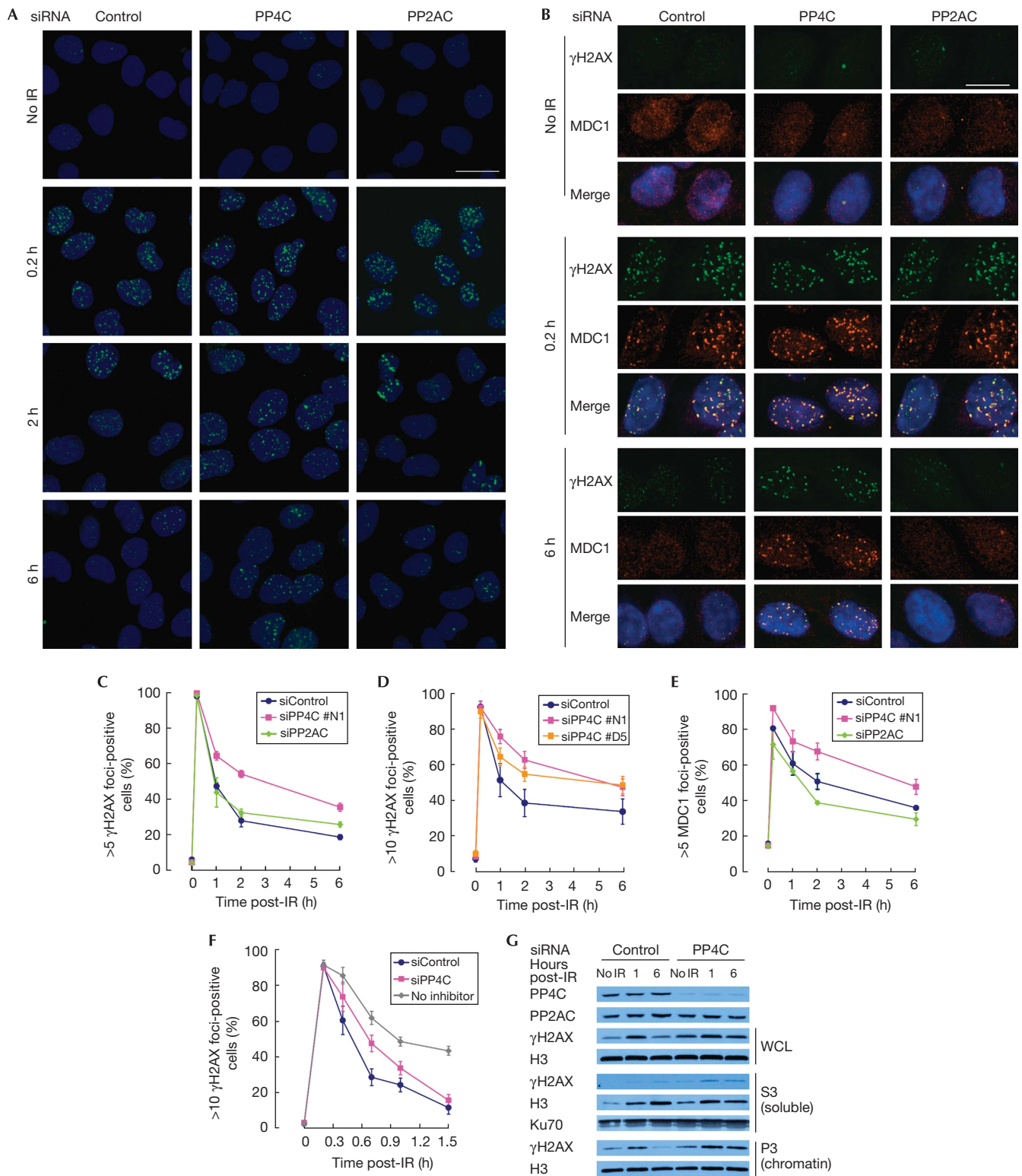


Fig 2 | PP4 reduces γ H2AX independently of a role in DNA repair *in vivo*. (A,B) U2OS cells were transfected with siRNAs against PP4C, PP2AC α/β (A), PP4R2 (B) or a non-targeting control sequence. Cells were irradiated with 10 Gy and collected at the indicated times after IR for immunoblotting with the indicated antibodies. Signal intensity was analysed using Image-J (<http://rsb.info.nih.gov/ij/>). Signal intensity of γ H2AX is normalized against that of histone H3. (C) Cells were irradiated with 50 Gy and collected at the indicated times after IR for neutral comet assays. A representative image of the nuclei is presented. (D) Quantification of the comet tail moments of the experiment in (C). Tail moments for each condition were calculated on a minimum of 75 cells for each data point, normalized against the average comet tail moment of the mock-irradiated control, and shown as a box-and-whisker plot. Outliers are indicated as dots. The ordinate is a square-root scale. Data were statistically analysed using the Wilcoxon test. *P*-values are adjusted for several comparisons with the Bonferroni method. **P* < 0.05; ***P* < 0.01; ****P* < 0.0001; NS, no significance. (E) U2OS cells transfected with siRNAs against either PP4C or a control sequence were irradiated with 10 Gy. At 1 h post-IR, the ATM (KU55933) and DNA-PK (KU57788) inhibitors were added to the tissue culture medium (*t* = 0). Samples were then collected at the indicated time points and processed for immunoblotting with the indicated antibodies. Signal intensity was analysed using Image-J. Signal intensity of γ H2AX is normalized against that of histone H3. ATM, ataxia telangiectasia mutated; DNA-PK, DNA-dependent protein kinase; H3, histone H3; IR, irradiation; siRNA, small interfering RNA.

were designed to silence the expression of both proteins. Using this strategy, siRNA-mediated depletion of PP4C and PP2AC α/β in U2OS cells decreased the levels of both catalytic subunits to about 20% of the control levels. Levels of γ H2AX were estimated by immunoblotting before or 1–8 h after a 10 Gy dose of X-rays. As shown in Fig 2A, depletion of PP4C and PP2AC each resulted in a marked increase in the total levels of γ H2AX in both non-

irradiated and irradiated cells. To control for off-target effects, we repeated the experiment using other siRNAs and obtained similar results (supplementary Fig S3 online). Depletion of PP4R2 also resulted in an increase in the total levels of γ H2AX (Fig 2B), placing PP4R2 as part of a PP4C-containing complex that regulates the levels of γ H2AX in human cells. Furthermore, irradiation of cells with a 10 Gy dose of X-rays did not induce



rapid apoptosis in PP4C- and PP2AC-depleted cells, suggesting that the persistence of γ H2AX was independent of apoptosis (supplementary Fig S4 online). To test whether this increase in phosphorylation was due to lingering DSBs imparted by a DNA repair defect, we examined DSB rejoining kinetics in control,

PP2AC- and PP4C-depleted cells by neutral comet assays. As shown in Fig 2C,D, PP2AC-silenced cells are mildly impaired in the repair of X-ray-induced DSBs, which is consistent with the previously described function of PP2AC in the repair of camptothecin-induced lesions (Chowdhury *et al*, 2005). By

Fig 3 | PP4 dephosphorylates γ H2AX at the sites of DNA damage. (A,B) U2OS cells transfected with siRNAs against PP4C, PP2AC α/β or a control sequence were irradiated with 1.5 Gy and processed for γ H2AX (A,B) and MDC1 (B) immunofluorescence and DAPI counterstaining at the indicated time points. Images were taken with a $\times 40$ objective (A) or with a $\times 63$ objective (B). Scale bar, 23 μ m (A) and 16 μ m (B). (C–F) Quantification of cells with >5 γ H2AX (C), >10 γ H2AX (D,F) and >5 MDC1 (E) foci. At least 300 cells were analysed per experiment. Cells were treated with KU55933 and KU57788 12 min post-IR (F). Error bars represent standard error of mean of independent duplicated experiments (C) or standard deviation of three independent experiments (D–F). A $\times 63$ oil immersion objective (C,E) or a $\times 40$ water immersion objective (D,F) was used. (G) U2OS cells transfected with siRNAs against PP4C or a control sequence were collected at the indicated time points immediately before (no IR), or 1 or 6 h after irradiation (10 Gy), then fractionated as described in Méndez & Stillman (2000) into whole-cell lysates (WCLs), nuclear soluble (S3) or chromatin (P3) fractions, and analysed by immunoblotting using the indicated antibodies. DAPI, 4,6-diamidino-2-phenylindole; H3, histone H3; IR, irradiation; MDC1, mediator of DNA damage checkpoint 1; siRNA, small interfering RNA.

contrast, PP4C-silenced cells underwent DNA repair as efficiently as control cells. These data suggest that silencing PP2AC might lead to lingering DSBs that could affect steady-state phosphorylation of H2AX in human cells. By contrast, PP4C reduces the levels of γ H2AX independently of a role in DNA repair.

PP4 participates in the dephosphorylation of H2AX

PP2A-type enzymes have been linked to γ H2AX through the regulation of ATM activity (Goodarzi *et al*, 2004). Therefore, we sought to test whether PP4 acts directly on γ H2AX or indirectly by promoting the activity of ATM or DNA-PK, the two main H2AX kinases (Stiff *et al*, 2004). For this purpose, we examined the turnover of γ H2AX after the combined inhibition of ATM and DNA-PK. In preliminary studies, we found that a combination of the ATM inhibitor KU55933 and the DNA-PKcs inhibitor (DNA-PKi) KU57788 suppressed the irradiation-induced formation of γ H2AX (supplementary Fig S5 online). Therefore, we treated siRNA-transfected cells with both inhibitors 60 min post-irradiation to inhibit the phosphorylation of H2AX, and monitored the decay of γ H2AX by immunoblotting. Using this experimental scheme, depletion of PP4C resulted in slower kinetics of H2AX dephosphorylation (Fig 2E). These results indicate that PP4C can bring about dephosphorylation of H2AX *in vivo*, independently of an effect on ATM and DNA-PK.

PP4 dephosphorylates γ H2AX at the sites of DNA lesions

To identify the pools of γ H2AX targeted by PP4, we assessed the kinetics of γ H2AX focus formation and dissolution by indirect immunofluorescence (Fig 3A). To support the γ H2AX data, we also examined MDC1 foci dynamics, as the recruitment of MDC1 to DSB sites occurs through a direct interaction with γ H2AX (Stucki *et al*, 2005; Fig 3B). MDC1 foci therefore represent a functional readout of γ H2AX at DSB sites. In contrast to the result shown in Fig 2A, γ H2AX foci diminished rapidly in both PP4C- and PP2AC-depleted cells (Fig 3A). However, as shown in Fig 3A and quantified in Fig 3C, PP4C-depleted cells showed a slower decrease in γ H2AX foci-positive cells than control-transfected cells during the recovery from irradiation, whereas depletion of PP2AC did not affect γ H2AX foci kinetics. The slower dissolution of γ H2AX foci in PP4C-depleted cells was observed with a second independent siRNA (Fig 3D) and was rescued by the introduction of an siRNA-resistant PP4C cDNA (supplementary Fig S6 online), confirming the specificity of the phenotype. In addition, MDC1 foci dynamics closely matched those of the γ H2AX foci (Fig 3B,E). We also examined the dissolution of irradiation-induced γ H2AX foci after the addition of the ATM (KU55933) and DNA-PK (KU57788) inhibitors to exclude the possibility that depletion of PP4 results in an increase in the activity of ATM or DNA-PK. As

shown in Fig 3F, we found that the depletion of PP4C slowed the rapid dissolution of γ H2AX foci. Finally, we present as supplementary information online data examining γ H2AX focus morphology in PP4-depleted cells that are also consistent with a delay in focus dissolution (supplementary Fig S7 online). From these observations, we conclude that PP4 could dephosphorylate γ H2AX at the sites of DNA damage, whereas PP2A might not have a principal function at these sites after treatment with irradiation. However, other mechanisms must also be important to remove this histone marker from the chromatin that surrounds the DSB.

Dephosphorylation of H2AX occurs in chromatin

The persistence of irradiation-induced phosphorylation of H2AX in PP4- or PP2A-depleted cells, as detected by immunoblotting (Fig 2), conflicts with our observation that dissolution of γ H2AX foci still occurs in those cells, despite being slowed in the case of PP4. As the removal of γ H2AX from repaired chromatin is most likely to be the result of the combined action of phosphatases and histone exchange (Heo *et al*, 2008), we assessed whether the lingering γ H2AX observed in PP4-depleted cells is found in the nucleoplasm or associated with the chromatin after cell fractionation (Méndez & Stillman, 2000). We monitored the distribution of histone H3 to estimate nucleosome eviction or exchange. In the absence of irradiation, neither histone H3 nor γ H2AX was detected in the nuclear soluble fraction of control-transfected cells (supplementary Fig S8 online). After irradiation, or in PP4C-depleted cells, we observed an increase in γ H2AX and histone H3 in the soluble fraction, suggesting that γ H2AX stimulates histone exchange, as recently shown (Fig 3G; Heo *et al*, 2008). Nevertheless, we found that most of the persistent γ H2AX seen in PP4C-depleted cells remained associated with the chromatin fraction, despite the detectable increase in histone exchange or eviction (Fig 3G). On the basis of these results, we conclude that PP4 dephosphorylates γ H2AX primarily in the chromatin rather than in the nucleoplasm. A surprising corollary to these results is that recycling γ H2AX into chromatin might be an important step before its dephosphorylation. Indeed, as extensive chromatin remodelling and nucleosome eviction occurs during DSB repair, we propose that cells might have co-opted this process to promote the rapid removal of γ H2AX and dephosphorylation.

PP4 promotes recovery from the G2/M checkpoint arrest

The observation that focused dissolution of MDC1 is slowed after the depletion of PP4C suggests that PP4 might antagonize checkpoint signalling by stimulating focus disassembly at the sites of DNA damage. This possibility echoes the situation in yeast, in which Pph3 promotes G2/M checkpoint recovery (Keogh *et al*, 2006). Therefore, we established a system that monitors recovery

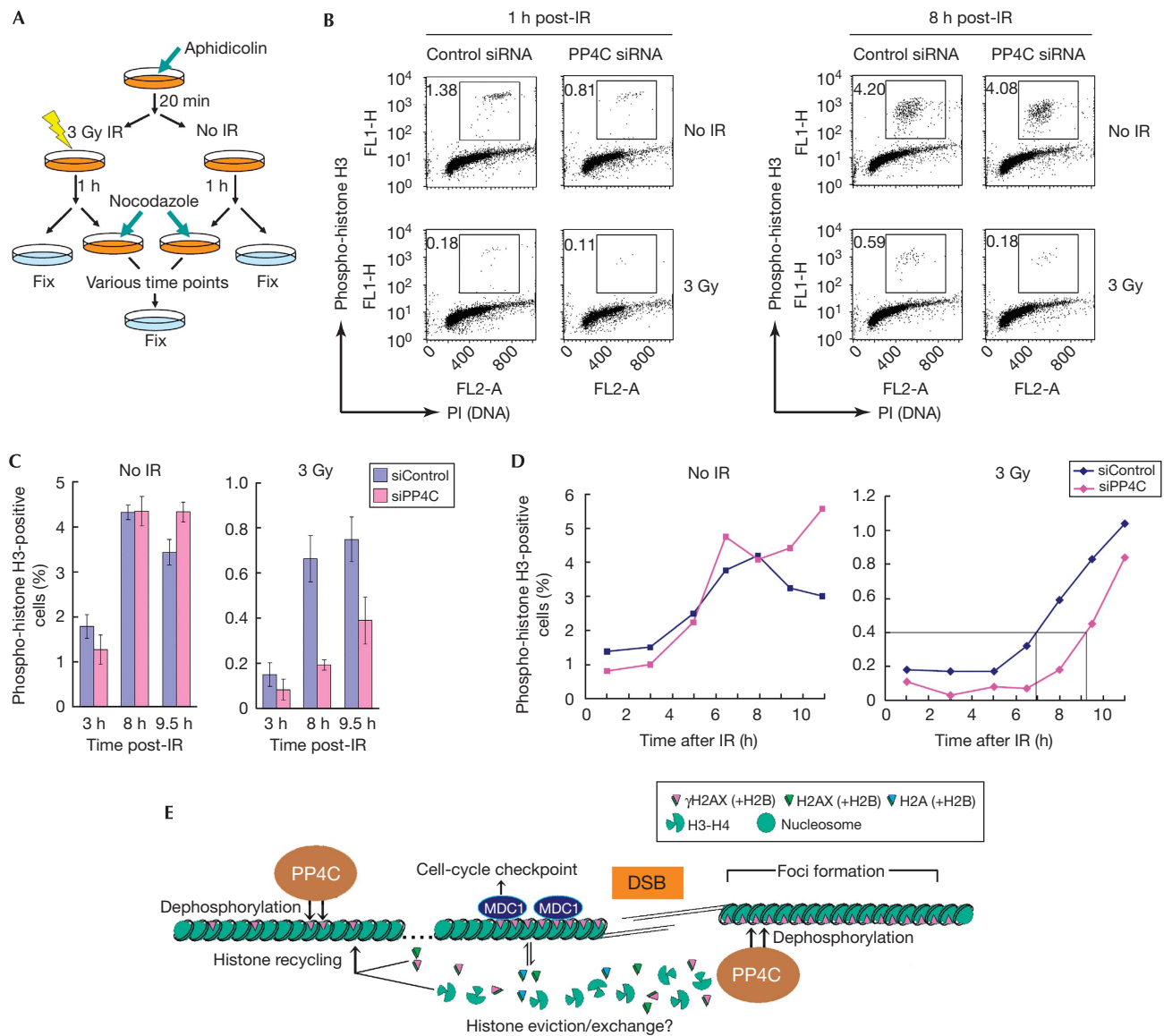


Fig 4 | PP4 promotes recovery from the G2/M checkpoint arrest. (A) Schematic diagram of the checkpoint recovery experiment. S-phase cells were first arrested by incubation with aphidicolin, then mock-treated (No IR) or irradiated with an X-ray dose of 3 Gy. At 1 h post-treatment, nocodazole was added to the media and cells were fixed at various time points for processing by flow cytometry. (B) U2OS cells transfected with siRNAs against PP4C or a non-targeting control sequence were collected 1 and 8 h after mock (No IR) or 3 Gy irradiation and processed for flow cytometry with an antibody against phospho-histone H3 and propidium iodide (PI). The boxes represent the mitotic cells. (C) U2OS cells transfected with siRNAs against PP4C or a non-targeting control sequence were mock-treated (No IR) or irradiated (3 Gy), and processed as described in (A). The percentage of mitotic cells (as determined by phospho-histone H3 staining) was calculated for each indicated time point. The experiment was repeated three times and the error bars represent the standard deviation. (D) Percentage of mitotic cells (as determined by phospho-histone H3 staining) calculated for each time point for the mock-irradiated (No IR, left) or irradiated (3 Gy, right) samples. The onset of mitosis represented by the intersecting lines was arbitrarily fixed at 0.4%. (E) Model of action of PP4 and dephosphorylation of γ H2AX. IR, irradiation; siRNA, small interfering RNA.

from the G2/M arrest after irradiation treatment (Fig 4A). By using this experimental scheme, we find that the percentage of phospho-histone H3-positive cells 1 h post-irradiation is comparable among control and PP4C siRNA-transfected cells, indicating that PP4 is not involved in the initiation of the G2/M checkpoint (Fig 4B,C). However, at later time points, we observed that control cells began entering mitosis 7 h post-irradiation, whereas PP4C-

depleted cells began entering mitosis more than 9 h after the initial arrest (Fig 4D; supplementary Fig S9 online). Seen from another angle, at the 8 h post-irradiation time point, PP4C-depleted cells showed a 3.3-fold reduction in the number of cells that entered mitosis (Fig 4B,C). These data indicate that PP4 has an important and evolutionarily conserved function during recovery from checkpoint arrest.

In conclusion, our results indicate that PP4 is a γ H2AX phosphatase in human cells that acts on γ H2AX not only at chromatin surrounding DNA damage but also at intact chromatin and that it is required for recovery from the DNA damage checkpoint (Fig 4E). The function of PP4 in the dephosphorylation of γ H2AX is therefore evolutionarily conserved, whereas that of PP2A seems to have been acquired during eukaryotic evolution (or lost by budding yeast). We made the surprising observation that PP4 and PP2A do not act redundantly. PP4 dephosphorylates γ H2AX at irradiation-induced DSBs, whereas PP2A has a minimal function at those sites. Our finding conflicts with a previously published report (Chowdhury *et al*, 2005), in which PP2AC-depleted cells showed persistent γ H2AX foci after treatment with camptothecin (a topoisomerase I inhibitor). Here, we note the possibility that PP4 and PP2A might respond to different types of DNA damage. In addition, the delayed kinetics of dissolution of γ H2AX foci, which was seen by Chowdhury *et al* (2005) in PP2AC-depleted cells, could also simply be due to the observed DNA repair defect. Future work will be aimed at deciphering whether PP4 and PP2A have distinct functions in the turnover of H2AX phosphorylation and also how they cooperate with the chromatin remodelling processes that act at the sites of DNA damage to control the DNA damage response.

METHODS

RNA interference. All siRNA transfections were performed using Dharmafect 1 (ThermoFisher; Waltham, MA, USA). All experiments were performed from 32 to 48 h post-siRNA transfection; siRNA sequences are described in the supplementary information online.

Western blotting. Nitrocellulose membranes were stained with mouse anti- γ H2AX (Upstate; Temecula, CA, USA; clone JBW301, at 1:5000 dilution in 3% BSA in PBS), rabbit anti-PP4C (Bethyl; Montgomery, TX, USA; A300-835A, 1:4000), rabbit anti-PP4R2 (Bethyl; A300-838A, 1:2000), mouse anti-PP2AC (BD Biosciences; San Jose, CA, USA; clone 46, 1:2000) and rabbit anti-histone H3 (Abcam; Cambridge, UK; ab1791, 1:20,000).

Immunofluorescence. U2OS human osteosarcoma (ATCC HTB-96) cells were grown on glass coverslips, fixed with methanol at -20°C , and then permeabilized with acetone at -20°C . Blocking, incubations with mouse anti- γ H2AX (1:10,000; Upstate; clone JBW301), sheep anti-MDC1 (1:1000; AbD Serotec; AHP799) and secondary antibodies and washes were carried out in ADB (3% normal goat serum, 0.1% Triton X-100 in PBS). DNA was counterstained with 4,6-diamidino-2-phenylindole and coverslips were mounted with Prolong Gold (Invitrogen; Eugene, OR, USA). Images were taken using a Leica DMIRE2 microscope equipped with a $\times 63$ oil immersion objective, or a Zeiss Axiovert200M microscope equipped with a $\times 20$ objective or $\times 40$ water immersion objective, a CSU10 spinning disc confocal unit (Yokogawa; Tokyo, Japan) and a C9100-12 camera (Yokogawa) using Volocity software (Improvision; Coventry, UK).

G2/M checkpoint recovery assay. Cells were first exposed to 5 $\mu\text{g}/\text{ml}$ aphidicolin, a DNA polymerase inhibitor, to prevent progression to S phase. Next, cells were irradiated with a dose of 3 Gy, and 1 h post-irradiation 100 ng/ml nocodazole was added to the media to capture cells entering mitosis. Cells were fixed with 2% paraformaldehyde at various time points, permeabilized with 90% methanol and blocked with fluorescence-activated cell sorting incubation buffer (0.5% BSA in PBS) for 10 min. Cells

were then stained with anti-phospho-histone H3 (Ser10) and fluorescein isothiocyanate-conjugated donkey anti-mouse IgG (Jackson ImmunoResearch; West Grove, PA, USA) and counterstained with propidium iodide (Sigma-Aldrich; St Louis, MO, USA). More than 10,000 cells per condition were analysed by flow cytometry (FACSCalibur; Becton Dickinson; Franklin Lakes, NJ, USA). Data were analysed by Cell Quest Pro (Becton Dickinson).

Phosphatase assays. For histone dephosphorylation, eluted phosphatases were first preincubated in 35 μl of reaction buffer (50 mM Tris-Cl pH 7.2, 0.1 mM CaCl_2 , 5 mM MnCl_2 and 0.2 mg/ml BSA) for 10 min at 30°C . Acid-extracted histones were then added and phosphatase reactions were incubated at 30°C for 1 h.

Neutral comet assay (single-cell gel electrophoresis). Neutral comet assays were performed on cells exposed to a dose of 50 Gy X-ray. Assays were carried out using the Comet Assay system (Trevigen; Gaithersburg, MD, USA), according to the manufacturer's instructions with a minor modification: samples were treated with RNaseI and stained with propidium iodide. In total, 75 cells were analysed per sample using Scion Image with the comet assay macro, scion_comet1.3 (Helma & Uhl, 2000) for comet tail moment.

Supplementary information is available at *EMBO reports* online (<http://www.emboreports.org>).

ACKNOWLEDGEMENTS

We thank B. Raught, M. Downey and R. Szilard for their inputs on the paper. We are also grateful to KuDOS Pharmaceuticals for providing DNA-PK and ATM inhibitors. This study was supported by grants from the Canadian Cancer Society to D.D., and the Terry Fox Foundation to A.-C.G. S.N. is a Gail Posluns Fellow and was supported by the Mitsubishi Pharma Research Foundation and the Japan Leukemia Research Fund. G.I.C. was supported by the Ontario Student Opportunities Trust Fund. D.D. and A.-C.G. are both Canada Research Chairs (Tier II).

CONFLICT OF INTEREST

The authors declare that they have no conflict of interest.

REFERENCES

- Brewis ND, Street AJ, Prescott AR, Cohen PT (1993) PPX, a novel protein serine/threonine phosphatase localized to centrosomes. *EMBO J* **12**: 987–996
- Celeste A, Fernandez-Capetillo O, Kruhlak MJ, Pilch DR, Staudt DW, Lee A, Bonner RF, Bonner WM, Nussenzweig A (2003) Histone H2AX phosphorylation is dispensable for the initial recognition of DNA breaks. *Nat Cell Biol* **5**: 675–679
- Chowdhury AK, Watkins T, Parinandi NL, Saatian B, Kleinberg ME, Usatyuk PV, Natarajan V (2005) Gamma-H2AX dephosphorylation by protein phosphatase 2A facilitates DNA double-strand break repair. *Mol Cell* **20**: 801–809
- Cohen PT, Brewis ND, Hughes V, Mann DJ (1990) Protein serine/threonine phosphatases; an expanding family. *FEBS Lett* **268**: 355–359
- Gavin AC *et al* (2002) Functional organization of the yeast proteome by systematic analysis of protein complexes. *Nature* **415**: 141–147
- Gingras AC, Caballero M, Zarske M, Sanchez A, Hazbun TR, Fields S, Sonenberg N, Hafen E, Raught B, Aebersold R (2005) A novel, evolutionarily conserved protein phosphatase complex involved in cisplatin sensitivity. *Mol Cell Proteomics* **4**: 1725–1740
- Goodarzi AA, Jonnalagadda JC, Douglas P, Young D, Ye R, Moorhead GB, Lees-Miller SP, Khanna KK (2004) Autophosphorylation of ataxia-telangiectasia mutated is regulated by protein phosphatase 2A. *EMBO J* **23**: 4451–4461
- Harper JW, Elledge SJ (2007) The DNA damage response: ten years after. *Mol Cell* **28**: 739–745

- Helma C, Uhl M (2000) A public domain image-analysis program for single-cell gel-electrophoresis (comet) assay. *Mutat Res* **466**: 9–15
- Heo K, Kim H, Choi SH, Choi J, Kim K, Gu J, Lieber MR, Yang AS, An W (2008) FACT-mediated exchange of histone variant H2AX regulated by phosphorylation of H2AX and ADP-ribosylation of Spt16. *Mol Cell* **30**: 86–97
- Ho Y *et al* (2002) Systematic identification of protein complexes in *Saccharomyces cerevisiae* by mass spectrometry. *Nature* **415**: 180–183
- Keogh MC *et al* (2006) A phosphatase complex that dephosphorylates gammaH2AX regulates DNA damage checkpoint recovery. *Nature* **439**: 497–501
- Linger JG, Tyler JK (2007) Chromatin disassembly and reassembly during DNA repair. *Mutat Res* **618**: 52–64
- Méndez J, Stillman B (2000) Chromatin association of human origin recognition complex, cdc6, and minichromosome maintenance proteins during the cell cycle: assembly of prereplication complexes in late mitosis. *Mol Cell Biol* **20**: 8602–8612
- Rogakou EP, Pilch DR, Orr AH, Ivanova VS, Bonner WM (1998) DNA double-stranded breaks induce histone H2AX phosphorylation on serine 139. *J Biol Chem* **273**: 5858–5868
- Rogakou EP, Boon C, Redon C, Bonner WM (1999) Megabase chromatin domains involved in DNA double-strand breaks *in vivo*. *J Cell Biol* **146**: 905–916
- Ronne H, Carlberg M, Hu GZ, Nehlin JO (1991) Protein phosphatase 2A in *Saccharomyces cerevisiae*: effects on cell growth and bud morphogenesis. *Mol Cell Biol* **11**: 4876–4884
- Stiff T, O'Driscoll M, Rief N, Iwabuchi K, Löbrich M, Jeggo PA (2004) ATM and DNA-PK function redundantly to phosphorylate H2AX after exposure to ionizing radiation. *Cancer Res* **64**: 2390–2396
- Stucki M, Clapperton JA, Mohammad D, Yaffe MB, Smerdon SJ, Jackson SP (2005) MDC1 directly binds phosphorylated histone H2AX to regulate cellular responses to DNA double-strand breaks. *Cell* **123**: 1213–1226
- Tung HY, Alemany S, Cohen P (1985) The protein phosphatases involved in cellular regulation. 2. Purification, subunit structure and properties of protein phosphatases-2A0, 2A1, and 2A2 from rabbit skeletal muscle. *Eur J Biochem* **148**: 253–263
- Zhou J, Pham HT, Walter G (2003) The formation and activity of PP2A holoenzymes do not depend on the isoform of the catalytic subunit. *J Biol Chem* **278**: 8617–8622



EMBO reports is published by Nature Publishing Group on behalf of European Molecular Biology Organization. This article is licensed under a Creative Commons Attribution-Noncommercial-No Derivative Works 3.0 License. [<http://creativecommons.org/licenses/by-nc-nd/3.0>]